ADVANCED MATERIALS INTERFACES
www.advmatinterfaces.de

Can Metals Other than Au be Used for Large Area Exfoliation of MoS_2 Monolayers?

*Ammon Cody Johnston and Saiful I. Khondaker**

Au-mediated exfoliation of 2D transition-metal dichalcogenides (TMDs) has received significant attention due to its ability to produce large-area monolayer (ML) flakes. This process has been attributed to strong TMD/Au binding energy (BE) as well as the uniform strain between the TMDs and Au. However, large-area exfoliation of TMDs with other metals that have even stronger theoretical BE than Au/TMD is not successful, leading to question whether the BE plays any role in the exfoliation process. Here, successful demonstration of large-area ML MoS_2 using Cu, Ni, and Ag with various predicted strain, including Pd with almost no strain, but stronger BE than Au/MoS_2 is demonstrated. Optical micrographs show MoS_2 flakes with 100s of μm in size with a yield of several tens to hundreds of ML flakes per exfoliation. Photoluminescence and Raman spectroscopy confirm the ML nature of the flakes, while electrical transport measurements show mobilities of ≈6 $cm^2 V^{-1} s^{-1}$ with a current on-off ratio ≈10^8 consistent with high-quality ML MoS_2. Given that MoS_2 can be exfoliated with metals that have strong BE irrespective of their strain values suggests that BE is the primary mechanism in successful exfoliation of large-area ML MoS_2.

1. Introduction

Since the exfoliation of monolayer (ML) graphene[1] by micromechanical exfoliation process (i.e., scotch tape method), it has been routinely used by numerous researchers to produce ML flakes of diverse 2D materials for studying novel physics, and to demonstrate applications in electronics and optoelectronics devices including heterojunctions.[2–8] However, this technique suffers from low yield and is limited to producing a few micron sized flakes, therefore not scalable to produce large-area ML flakes. Recently, Au-mediated exfoliation[9–12] has been introduced as a way to produce high quality large-area ML 2D transition-metal dichalcogenides (TMDs) and other 2D materials with lateral dimensions of 100s of μm in size.[11] Flakes produced via this method have already been used in multiple applications including gas sensing,[13] photodetection,[14,15] and heterostructure arrays.[16,17] It has been claimed that the stronger Au/2D TMD interfacial interaction or binding energy (BE) of the top layer overcomes the weaker interlayer van der Waals (VdW) forces between the top layers and subsequent layers in TMD materials, thereby leaving behind large-area ML flakes.[9,12,18]

The origin of stronger Au/2D TMDs is due to the well-known affinity of Au towards chalcogen atoms and is well studied in self-assembling monolayers (SAM) formation.[19–22] Theoretical and experimental studies have shown that there are other metals which possess similar affinity to chalcogens.[23] Although reproducible SAMs can be obtained on Au, it has also been demonstrated that several other metals (e.g., Pd, Cu, Ni, Ag) can form excellent SAMs implying that these metals also have stronger BE with 2D TMDs.[23] Indeed, Au has one of the smallest predicted BEs with TMDs (Au/MoS_2s predicted BE is ≈–0.2 eV[24]) among metals, suggesting that many metals other than Au could be used in exfoliation. However, successful exfoliation of large-area ML 2D TMDs using other metals has remained elusive. This raises a fundamental question: is this interfacial interaction, or BE, between Au and other metals with 2D TMDs indeed an important factor for the large-area exfoliation? A few theoretical studies suggested that when Au is deposited on MoS_2, a bi-axial tensile strain is induced in the plain of the top MoS_2 layer to compensate for their large lattice mismatch.[25,26] Some studies suggested that both the BE and uniform strain produced by Au/2D material's lattice mismatch is responsible[10] while other studies suggested that the Au/chalcogen interaction (i.e., BE) is not the determining factor for exfoliation. Instead, uniform strain is the determining factor and other metals that do not produce such uniform strain are unable to exfoliate large-area ML TMDs.[26,27] Given that there are more than 800 layered crystals are predicted to form ML flakes by exfoliation[28] of which only ≈40 2D materials have been realized,[12] a study and demonstration of other metal-mediated large-area exfoliation is important for the practical realization of many future 2D materials.

Here, we demonstrate successful exfoliation of large-area ML MoS_2 using Pd, Cu, Ni and Ag metals all of whom have stronger predicted BE than Au with MoS_2. On the other hand,

A. C. Johnston, S. I. Khondaker
Department of Physics and NanoScience Technology Center
University of Central Florida
Orlando, FL 32816, USA
E-mail: saiful@ucf.edu
S. I. Khondaker
Electrical & Computer Engineering
University of Central Florida
Orlando, FL 32816, USA

The ORCID identification number(s) for the author(s) of this article can be found under https://doi.org/10.1002/admi.202200106.

DOI: 10.1002/admi.202200106

Pd has negligible strain while Cu has similar, and Ni and Ag has greater predicted strain than Au with MoS_2.[24,25] These metals were directly evaporated onto MoS_2 bulk crystal, and the metal layer was then exfoliated away from the bulk source with ML MoS_2 attached and placed on a clean Si/SiO_2 substrate. The metal was chemically removed using the appropriate etchants. We show for the first time that Pd, Cu, Ni, and Ag can exfoliate high quality ML MoS_2 flakes that are 100s of μm in size, with a yield of several tens to hundreds of ML flakes per exfoliation that is highly reproducible over multiple iterations. Photoluminescence (PL) and Raman spectroscopy (RS) confirm the ML nature of the flakes with an A peak of ≈1.9 eV and a $\Delta \approx 19\ cm^{-1}$ between the E' and A_1' peaks. Electrical transport measurements show device mobilities of ≈6 $cm^2\ V^{-1}\ s^{-1}$ with a current on–off ratio ≈10^8, consistent with high-quality scotch tape exfoliated ML MoS_2 devices fabricated under identical conditions. Given that MoS_2 can be exfoliated with metals that have strong predicated BE independent of their strain values, including metals that have negligible strain, suggest that that BE is the primary mechanism in successful exfoliation of large-area ML MoS_2. As there are numerous layered crystals which are being grown from which 2D materials can be exfoliated, this study will help guide successful exfoliation of many new exotic large-area 2D materials for fundamental discovery and novel applications.

2. Results and Discussions

For this work, we followed a similar technique detailed in Desai et al.[10] except that Au was replaced with another metal source. To determine if uniform strain or BE is the driving factor in metal exfoliation, we used Pd, Cu, Ni, Mo, Al, and Ag that have different predicted strain and BE with MoS_2 to exfoliate large-area ML MoS_2.[24,25] The schematic of a typical exfoliation process is provided in **Figure 1**. For each metal-mediated exfoliation, a bulk MoS_2 flake was first exfoliated onto a Kapton tape and a thin film of metal was deposited by e-beam evaporation. Thermal release tape was then used to peel off the top layer of MoS_2. The metal/MoS_2 is then lightly pressed onto a Si/SiO_2 substrate followed by the removal of thermal release tape and metal thin film (see Experimental Section for more details).

We first exfoliated using Pd, that has a large theoretical BE (–0.69 eV[25]) and negligible (up to 5× less than Au)[24] strain with MoS_2. **Figure 2**a show an image of the first successful Pd-exfoliated large-area ML MoS_2 sample on Si/SiO_2 substrate, identified by optical contrast as described in literature,[29] with lateral dimensions of 140 × 200 μm. Additional flakes can be seen in Figure S1 (Supporting Information). Figure 1b shows a histogram of flake lateral dimension over 4 different Pd exfoliations with an average yield of 26.5 ± 4.99 ML flakes per exfoliation demonstrating the highly reproducible nature of this exfoliation. Although the majority of the exfoliated flakes are ML, we also found that the exfoliation produces a few (≈1–3 flakes per exfoliation) bi-layer to multilayer flakes (see Figure S1c, Supporting Information). The ML flake dimensions, determined optically, had an average lateral dimension of 47.13 ± 3.23 μm, although some flakes are hundreds of microns in size (see Figure S1a, Supporting Information). Despite Pd/MoS_2 having been predicted to have 5× less strain[24,27] than Au/MoS_2, Pd exfoliation yields results comparable or better than Au reported in literature,[10,30,31] suggesting that strain may not be the leading cause in the successful metal exfoliation of large-area ML MoS_2. If uniform strain was the determining factor in exfoliation, then we would not be able to use Pd to exfoliate large-area ML MoS_2 as Pd/MoS_2 has negligible predicted strain. Instead, our results suggest that having a strong BE is the reason for the successful exfoliation, as the predicted BE of Pd/MoS_2 is larger than Au/MoS_2's BE.

Prior to testing other metals to further confirm that BE is the driving factor behind metal exfoliation, we carried out detailed optical and electrical characterizations to determine the quality of Pd-exfoliated ML MoS_2 flakes. Raman spectroscopy (RS) was used to confirm ML nature of MoS_2 (Figure 2c). The two prominent peaks correspond to the in-plane ($E' = 386.2\ cm^{-1}$) and out-of-plane ($A_1' = 405.4\ cm^{-1}$) vibrational modes of Mo and S. These peaks have a frequency difference of $\Delta = 19.2\ cm^{-1}$, confirming a ML flake.[7,32,33] The E' and A_1' peak positions and FWHM are consistent with our control Au and scotch tape exfoliated MoS_2 samples (see Figure S2, Supporting Information), suggesting high quality ML MoS_2 flakes. The Photoluminescence (PL) spectra (Figure 2d) agrees with the RS findings, the ML MoS_2 PL has an A peak at about 1.9 eV that is consistent with

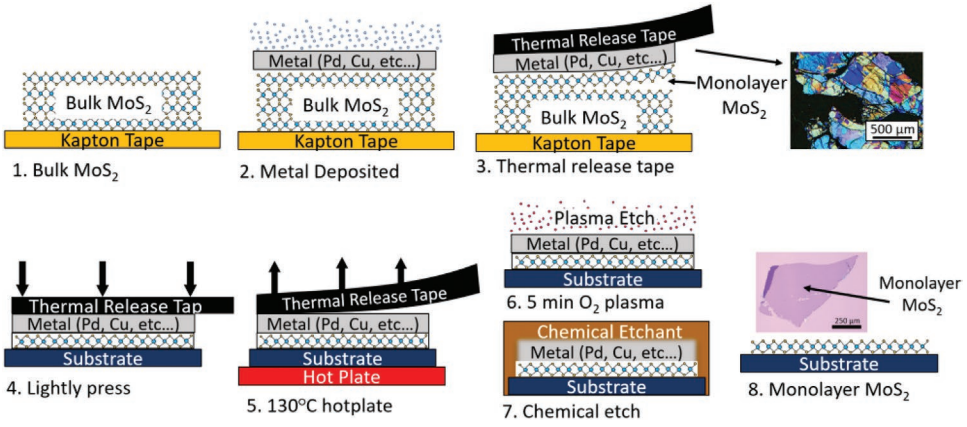

Figure 1. Step-by-step schematic of metal-mediated exfoliation method for MoS_2 monolayers. Picture inserts of MoS_2 on Pd (top 500 μm bar) and ML MoS_2 on SiO_2 (bottom 250 μm bar).

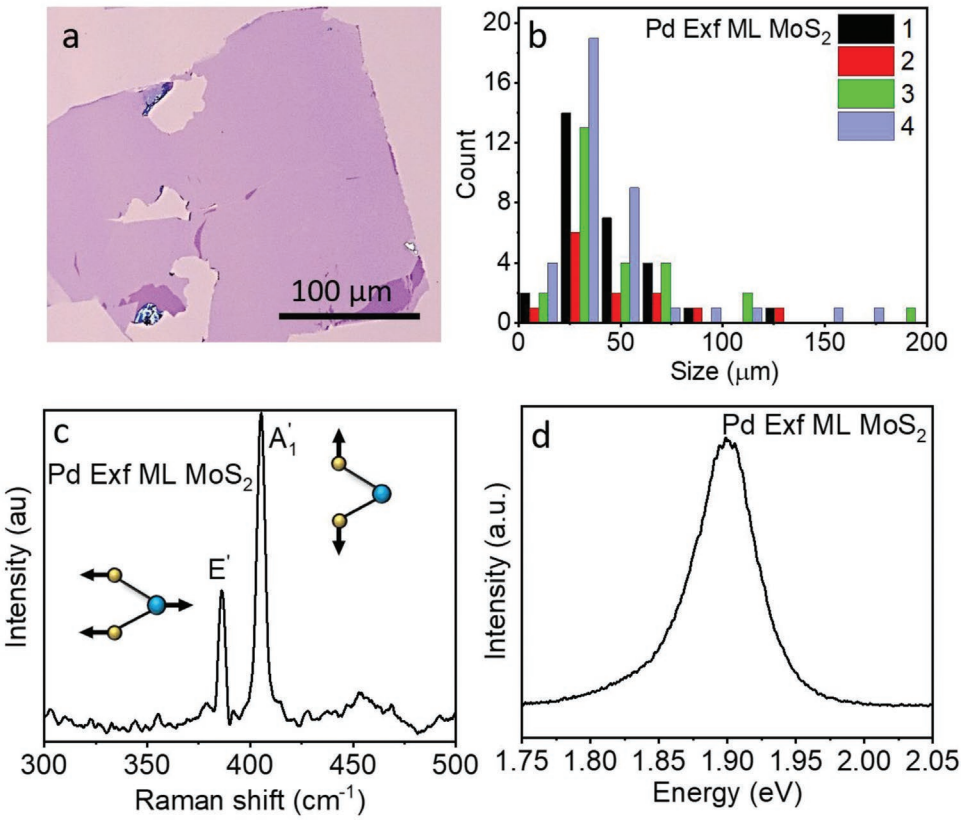

Figure 2. Pd-mediated exfoliation of ML MoS_2. a) Optical image, b) yield (flake counts and size in µm) of 4 Pd-mediated exfoliations, c) Raman spectra with $\Delta \approx 19.2$ cm^{-1}, and d) photoluminescence peak.

literature.[34] We also performed Raman peak position mapping for both the E' and A_1' peaks that can be seen in Figure S3 (Supporting Information) and both peaks show spatial uniformity in peak position across the ML flake. The agreement in the Raman and PL findings strongly suggest that the Pd exfoliation produces high-quality crystalline ML MoS_2.

Electrical characterization of Pd exfoliated MoS_2 flakes on Si/SiO_2 substrate were performed to further confirm the high-quality of the ML MoS_2 flakes (**Figure 3**b inset shows a schematic of the device). Figure 3a show current (I_{ds}) versus voltage (V_{ds}) (output characteristics) curves at different gate voltages (V_g) while Figure 3b shows I_{ds} versus V_g (transfer characteristics) curves of a representative Pd-exfoliated MoS_2 device. The increase of drain current with V_g is consistent with *n*-type field effect transistor (FET) behavior typically observed for MoS_2 devices. The output characteristics at different V_g shows linear behavior at low bias (Figure S4, Supporting Information) suggesting an Ohmic contact. The transfer characteristics of the same device taken at a $V_{ds} = 1$ V (Figure 3b) show the current increased by almost 8 orders of magnitude giving a current on-off ratio (I_{on}/I_{off}) of $\approx 10^8$, comparable with many of the best optimized ML MoS_2 devices.[35–38] The field effect

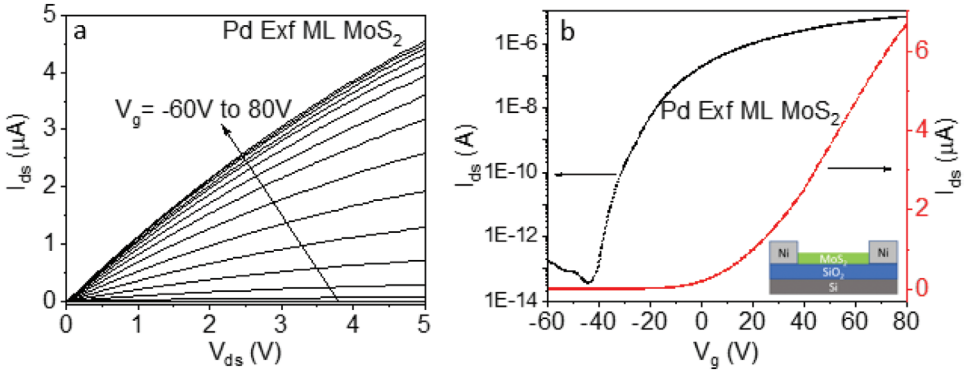

Figure 3. Pd-mediated exfoliated ML MoS_2 back-gate device a) I_{ds}–V_{ds} curve measured at different V_g from –60 to 80 V with 10 V step, and b) I_{ds}–V_g curve measured from –60 to 80 V at a fixed $V_{ds} = 1$ V. Left curve (black) is in log scale, while right curve (red) is in linear scale.

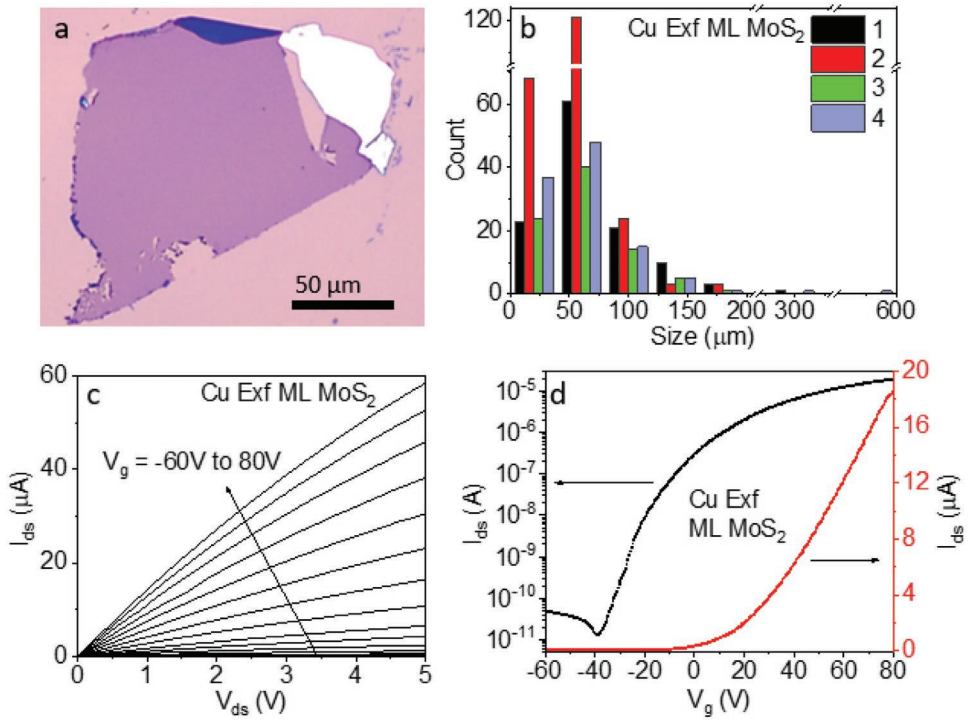

Figure 4. Cu-mediated exfoliated ML MoS_2. a,b) Optical image yields of 4 Cu-mediated exfoliations, c) I_{ds}–V_{ds} curve measured from 0 to 5 V, and d) I_{ds}–V_g curve measured from –60 to 80 V. Left curve (black) is in log scale, while right curve (red) is in linear scale.

mobility of the device was calculated to be 5.7 cm^2 V s^{-1} using $\mu = (L/WC_gV_{ds})$ (dI_{ds}/dV_g), were L = 3.9 μm and W = 5.5 μm being the channel length and width, $C_g = \varepsilon_0\varepsilon_r A/d$ is the capacitance per unit length of the gate dielectric (SiO_2). Similar results were obtained for two other flakes that we have measured. These results are consistent with scotch tape exfoliated ML MoS_2 back-gated devices fabricated on Si/SiO_2 substrates reported in the literatures,[32,36,39–42] suggesting that the crystalline quality of our Pd exfoliated flakes are comparable to that of conventional micromechanically exfoliated flakes.

We then proceeded to exfoliated MoS_2 using Cu to further understand the role of BE in ML MoS_2 exfoliation. Cu/MoS_2 has a larger predicted BE (–0.4 eV)[25] than Au/MoS_2, but both share a similar predicted strain.[28] Using Cu as the exfoliation metal produced an average 134.5 ± 29.8 ML MoS_2 flakes per exfoliation (**Figure 4**a) with an average area of 62.96 ± 1.86 μm (Figure 4b) and some flakes with dimensions greater than 500 μm (see Figure S5, Supporting Information). We verified the ML nature of our flakes by RS and find an E' peak at 386.2 cm^{-1} and a A_1' peak at 405.2 cm^{-1} that have a frequency difference of a Δ = 19.0 cm^{-1} (see Figure S6a, Supporting Information). PL has an A peak at ≈1.89 eV that is consistent with a ML flake (see Figure S6b, Supporting Information). RS and PL of Cu exfoliated ML MoS_2 flakes are near identical to Pd exfoliated flakes suggesting they are high-quality crystalline flakes. The output and transfer characteristics were measured for the Cu exfoliated MoS_2 flakes and measurements from a representative flake in shown in Figure 4c,d. The output of Cu exfoliated flakes suggests Ohmic contacts and shows increasing current with increasing V_{ds} typical of a n-type device. The transfer characteristics shows an on-current near 20 μA higher than many pristine ML MoS_2 devices.[39] We also find a I_{on}/I_{off} ratio is ≈10^6 and a mobility of 5.4 cm^2 V^{-1} s^{-1} similar to our high quality Pd exfoliated samples.

Next, we used Ni to exfoliate large-area ML MoS_2, as Ni/MoS_2 has a large predicted BE of –0.51 eV and a predicted strain larger than Au/MoS_2.[25] An optical image and a histogram can be seen in **Figure 5**a,b, respectively. The Ni exfoliated ML flakes have an average size of 143.36 ± 4.95 μm, larger than Pd or Cu exfoliated flakes, and produced an average of 181 ± 69 flakes per exfoliation comparable with to Cu exfoliation results. We verified the ML nature using RS, seeing a E' peak at 385.9 cm^{-1} and a A_1' peak at 405.5 cm^{-1} giving a Δ = 19.6 cm^{-1} (Figure S7, Supporting Information). The peak positions and measured FWHM verify ML nature and suggest highly crystalline flakes. We next exfoliated using Ag that has a predicted BE with MoS_2 of ≈–0.35 eV[25] and an optical picture of a representative flake is shown in Figure 5c. Figure 5d shows yield results of 14 ± 2 flakes per exfoliation and an average flake size of 95 ± 12.57 μm. We also used Al and Mo to exfoliate ML MoS_2 and their optical images are shown in Figure S8a,b (Supporting Information), respectively. Al has a predicted BE with MoS_2 of –0.3 eV[25] and a smaller predicted strain than Au/MoS_2[24] while the predicted BE and strain of Mo/MoS_2 is unavailable. The results of both exfoliations are shown in the histograms seen in Figure S8b (Supporting Information) (Al) and Figure S8d (Supporting Information) (Mo). Al and Mo resulted in 15 ± 4.78 and 18 ± 4.38 flakes per exfoliation respectively but had large flakes (up to ≈800 μm) that were broken or fracture into pieces < 5 μm, making them unsuitable for device applications. The cause of these fractures is not clear, but future process optimization may provide answers, as the large dimensions of these flakes are encouraging.

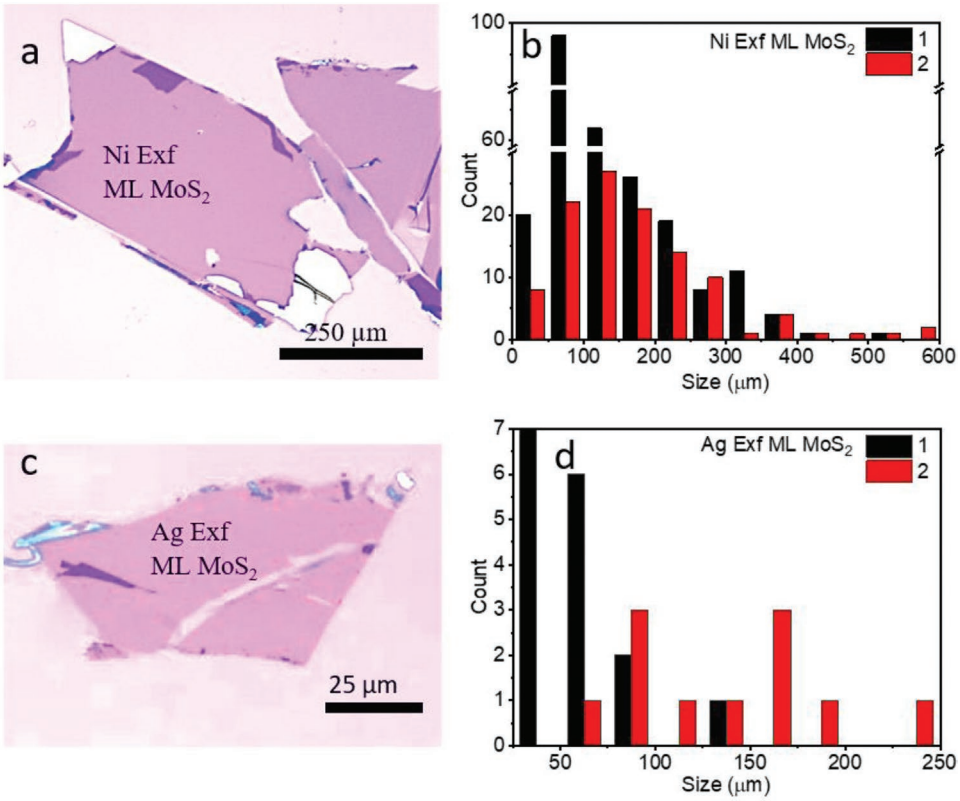

Figure 5. Ni-mediated exfoliated ML MoS_2. a,b) Optical image yields of two Ni-mediated exfoliations. Ag-mediated exfoliated ML MoS_2. c,d) Optical image and yields of two Ag-mediated exfoliations.

In a recent study, several metals including Au was used to exfoliate ML MoS_2, however, except Au, none of the other metals succeeded in large-area exfoliation.[27] The authors concluded that the BE is not the determining factor rather it was the uniform strain.[27] However, their metals (except Au) were oxidized before they came in contact with MoS_2 and MoS_2 is known to have a poor adhesion to oxides.[9] So we suggest that the increased oxidation from metals other than Au induces an overall metal/MoS_2 BE that is significantly less than the MoS_2/MoS_2 VdW's forces thus hindering large-area exfoliation of ML MoS_2. This is also supported by the SAM study where metals that are susceptible to oxidation needed to go through special handling (because oxides don't have good affinity to chalcogen).[23] In our case, the metal surface at metal/MoS_2 interface was not oxidized as we directly evaporated metals onto the MoS_2 in high-vacuum. As a result, the metal/MoS_2 BE remains intact. A recent density functional theory (DFT) calculation showed that the 2D crystal/Au interaction should be sufficient to overcome the interlayer attraction and facilitate exfoliating monolayers from a broad range of layered crystals[12] We argue that similar results should be true for other metal/2D TMDs.

3. Conclusions

In conclusion, we report a systematic study of large-area ML MoS_2 exfoliation using metals other than Au with BE greater than Au/MoS_2 BE with varying predicated strain. We show that Pd, Cu, Ni, and Ag can exfoliate large-area ML MoS_2 that are 100s of µm in size with a yield of several tens to hundreds of ML flakes per exfoliation. PL and RS characterizations confirm the ML and highly crystalline nature of the flakes with an A peak of ≈1.9 eV and a $\Delta \approx 19$ cm^{-1} between the E' (≈386 cm^{-1}) and A_1' (≈405.5 cm^{-1}) peaks. Electrical transport measurements of the exfoliated flakes are consistent with high-quality ML MoS_2[35–41] and show device mobilities of ≈6 cm^2 V^{-1} s^{-1} with a current on-off ratio ≈10^8. The fact that MoS_2 can be exfoliated with metals that have strong predicated BE independent of their strain values, including Pd that has negligible strain, suggest that that BE is the primary mechanism in successful exfoliation of large-area ML MoS_2 answering a fundamental question for the mechanism of large-area metal exfoliation process. As there are numerous layered crystals which are being grown from which 2D materials can be exfoliated, this study will help guide successful exfoliation of many new exotic large-area 2D materials for fundamental discovery and novel applications.

4. Experimental Section

Metal Exfoliation: The schematic of an exfoliation process is provided in Figure 1. Pd, Cu, Al, Mo, Au, or Ag thin metal film as a sacrificial layer to exfoliate large-area ML MoS_2 from a commercially available bulk MoS_2 crystal (SPI Supplies) was used. One exfoliation is defined as follows: A bulk flake is first exfoliated onto a glass side covered with double-sided Kapton tape. The sacrificial metal layer was deposited

through e-beam evaporation at a rate less than 0.5 A s^{-1}. The metal/MoS_2 was then exfoliated with a thermal release tape (Graphene Supermarket) and lightly pressed onto highly doped silicon wafer with a grown 250 nm SiO_2 capping layer. The thermal release tape was then removed on a hot plate at 130 °C. It was found that annealing MoS_2/metal while on SiO_2 at 150 °C for 20 min increased yield significantly by helping in adherence to the substrate.[42] Thermal tape residue was removed by mild oxygen plasma cleaning for 5 min while the MoS_2 was still protected by metal layer to avoid polymer contamination in the later wet etching steps. The metal layer was then etched away through wet etching technique. Different metals used in the exfoliation were etched using different metal etchants: Aqua regia (3:1:10-HCl: HNO_3:DI) was used for Pd removal, Cu etchant ($FeCl_3$) for Cu, Ni, and Mo removal, nitric acid (1:1-DI:HNO_3) for Ag removal, Al etchant Type A (7:2:1-H_3PO_4:CH_3COOH:HNO_3) (Al), and Au etchant (KI:I) for removal of Au and Ag. The etching was done for 4 min followed by cleaning in DI water (10 min), acetone dip (10 min), IPA rinse and finally drying with N_2 gas. The etching process did not etch the MoS_2 flakes and did not have any effect on the electrical properties and Raman spectra of ML MoS_2, consistent with previous reports where Au film was etched away during Au-mediated MoS_2 exfoliation.[10,43]

Material Characterization: After the etching the ML MoS_2 flakes were first optically characterized[29] for size and yield. The yield referred to the number of ML MoS_2 fakes derived from a single exfoliation. Raman and PL spectra were performed using a Horiba LabRAM HR Evolution spectrometer equipped with a scanning stage for mapping. A frequency doubled Nd:YAG laser with 532 nm excitation wavelength was used focused with 100× objective. Laser power was kept well below 1 mW in ambient conditions to avoid thermal or photodegradation, acquisition time and number of accumulations were optimized for each sample for higher throughput. All spectra were calibrated based on Si peak (520.7 cm^{-1}) and Gaussian or Lorentzian fitting was used for Raman band position analysis.

Device Fabrication and Characterization: Field effect transistors (FETs) devices with back-gate were fabricated on commercial highly p-doped Si with a 250 nm SiO_2 capping layer by using standard SEM e-beam lithography technique and e-beam deposition of 50 nm nickel to make source/drain contacts. The electrical transport measurements were carried out in ambient using a Keithley 2400 source meter and a DL instruments 1211 current preamplifier interfaced through LabView software. Highly doped Si was used as a back gate.

Supporting Information

Supporting Information is available from the Wiley Online Library or from the author.

Acknowledgements

This work was supported in part by the U.S. National Science Foundation (NSF) under Grant No. 1728309. Raman Spectroscopy and Atomic Force Microscopy images were taken with instruments supported by the U.S. NSF MRI Grant No. 1920050.

Conflict of Interest

The authors declare no conflict of interest.

Data Availability Statement

The data that support the findings of this study are available from the corresponding author upon reasonable request.

Keywords

2D materials, binding energy, interfacial strain, metal-mediated exfoliation, MoS_2

Received: January 16, 2022
Revised: February 25, 2022
Published online: March 20, 2022

[1] K. S. Novoselov, A. K. Geim, S. V. Morozov, D. Jiang, Y. Zhang, S. V. Dubonos, I. V. Grigorieva, A. A. Firsov, *Science* **2004**, *306*, 666.
[2] D. Moore, K. Jo, C. Nguyen, J. Lou, C. Muratore, D. Jariwala, N. R. Glavin, *Npj 2D Mater. Appl.* **2020**, *4*, 44.
[3] T. P. Darlington, C. Carmesin, M. Florian, E. Yanev, O. Ajayi, J. Ardelean, D. A. Rhodes, A. Ghiotto, A. Krayev, K. Watanabe, T. Taniguchi, J. W. Kysar, A. N. Pasupathy, J. C. Hone, F. Jahnke, N. J. Borys, P. J. Schuck, *Nat. Nanotechnol.* **2020**, *15*, 854.
[4] Y. Lee, S. J. Yun, Y. Kim, M. S. Kim, G. H. Han, A. K. Sood, J. Kim, *Nanoscale* **2017**, *9*, 2272.
[5] C. W. Tang, Z. He, W. B. Chen, S. Jia, J. Lou, D. V. Voronine, *Phys. Rev. B* **2018**, *98*, 041402.
[6] S. I. Khondaker, M. R. Islam, *J. Phys. Chem. C* **2016**, *120*, 13801.
[7] Q. H. Wang, K. Kalantar-Zadeh, A. Kis, J. N. Coleman, M. S. Strano, *Nat. Nanotechnol.* **2012**, *7*, 699.
[8] J. X. Liu, X. H. Chen, Q. Q. Wang, M. M. Xiao, D. L. Zhong, W. Sun, G. Y. Zhang, Z. Y. Zhang, *Nano Lett.* **2019**, *19*, 1437.
[9] G. Z. Magda, J. Peto, G. Dobrik, C. Hwang, L. P. Biro, L. Tapaszto, *Sci. Rep.* **2015**, *5*, 14714.
[10] S. B. Desai, S. R. Madhvapathy, M. Amani, D. Kiriya, M. Hettick, M. Tosun, Y. Zhou, M. Dubey, J. W. Ager3rd, D. Chrzan, A. Javey, *Adv. Mater.* **2016**, *28*, 4053.
[11] M. Velicky, G. E. Donnelly, W. R. Hendren, S. McFarland, D. Scullion, W. J. I. DeBenedetti, G. C. Correa, Y. Han, A. J. Wain, M. A. Hines, D. A. Muller, K. S. Novoselov, H. D. Abruna, R. M. Bowman, E. J. G. Santos, F. Huang, *ACS Nano* **2018**, *12*, 10463.
[12] Y. Huang, Y. H. Pan, R. Yang, L. H. Bao, L. Meng, H. L. Luo, Y. Q. Cai, G. D. Liu, W. J. Zhao, Z. Zhou, L. M. Wu, Z. L. Zhu, M. Huang, L. W. Liu, L. Liu, P. Cheng, K. H. Wu, S. B. Tian, C. Z. Gu, Y. G. Shi, Y. F. Guo, Z. G. Cheng, J. P. Hu, L. Zhao, G. H. Yang, E. Sutter, P. Sutter, Y. L. Wang, W. Ji, X. J. Zhou, et al., *Nat. Commun.* **2020**, *11*, 2453.
[13] H. Tabata, H. Matsuyama, T. Goto, O. Kubo, M. Katayama, *ACS Nano* **2021**, *15*, 2542.
[14] H. Y. Lan, Y. H. Hsieh, Z. Y. Chiao, D. Jariwala, M. H. Shih, T. J. Yen, O. Hess, Y. J. Lu, *Nano Lett.* **2021**, *21*, 3083.
[15] V. Krishnamurthi, M. X. Low, S. Kuriakose, S. Sriram, M. Bhaskaran, S. Walia, *ACS Appl. Nano Mater.* **2021**, *4*, 6928.
[16] V. Nguyen, H. Gramling, C. Towle, W. Li, D.-H. Lien, H. Kim, D. C. Chrzan, A. Javey, K. Xu, J. Ager, H. Taylor, *J. Micro Nano-Manuf.* **2019**, *7*, 041006.
[17] Z. Li, L. Ren, S. Wang, X. Huang, Q. Li, Z. Lu, S. Ding, H. Deng, P. Chen, J. Lin, Y. Hu, L. Liao, Y. Liu, *ACS Nano* **2021**, *15*, 13839.
[18] F. Liu, W. Wu, Y. Bai, S. H. Chae, Q. Li, J. Wang, J. Hone, X. Y. Zhu, *Science* **2020**, *367*, 903.
[19] H. Grönbeck, A. Curioni, W. Andreoni, *J. Am. Chem. Soc.* **2000**, *122*, 3839.
[20] H. Hakkinen, *Nat. Chem.* **2012**, *4*, 443.
[21] R. Jin, *Nanoscale* **2010**, *2*, 343.
[22] P. Maksymovych, D. C. Sorescu, J. T. Yates, *Phys. Rev. Lett.* **2010**, *97*, 146103.
[23] J. C. Love, L. A. Estroff, J. K. Kriebel, R. G. Nuzzo, G. M. Whitesides, *Chem. Rev.* **2005**, *105*, 1103.
[24] C. Gong, L. Colombo, R. M. Wallace, K. Cho, *Nano Lett.* **2014**, *14*, 1714.

[25] M. Farmanbar, G. Brocks, *Phys. Rev. B* **2016**, *93*, 085304.
[26] M. Ashton, J. Paul, S. B. Sinnott, R. G. Hennig, *Phys. Rev. Lett.* **2017**, *118*, 106101.
[27] M. Velický, G. E. Donnelly, W. R. Hendren, W. J. I. DeBenedetti, M. A. Hines, K. S. Novoselov, H. D. Abruña, F. Huang, O. Frank, *Adv. Mater. Interfaces* **2020**, *7*, 2001324.
[28] H. Sun, E. W. Sirott, J. Mastandrea, H. M. Gramling, Y. Zhou, M. Poschmann, H. K. Taylor, J. W. Ager, D. C. Chrzan, *Phys. Rev. Mater.* **2018**, *2*, 094004.
[29] H. Li, J. M. T. Wu, X. Huang, G. Lu, J. Yang, X. Lu, Q. H. Zhang, H. Zhang, *ACS Nano* **2013**, *7*, 10344.
[30] N. B. Guros, S. T. Le, S. Zhang, B. A. Sperling, J. B. Klauda, C. A. Richter, A. Balijepalli, *ACS Appl. Mater. Interfaces* **2019**, *11*, 16683.
[31] S. Zhang, H. M. Hill, K. Moudgil, C. A. Richter, A. R. Hight Walker, S. Barlow, S. R. Marder, C. A. Hacker, S. J. Pookpanratana, *Adv. Mater.* **2018**, *30*, 1802991.
[32] M. R. Islam, N. Kang, U. Bhanu, H. P. Paudel, M. Erementchouk, L. Tetard, M. N. Leuenberger, S. I. Khondaker, *Nanoscale* **2014**, *6*, 10033.
[33] X. Li, H. W. Zhu, *J. Materiomics* **2015**, *1*, 33.
[34] K. F. Mak, K. He, C. Lee, G. H. Lee, J. Hone, T. F. Heinz, J. Shan, *Nat. Mater.* **2013**, *12*, 207.
[35] Y. Yoon, K. Ganapathi, S. Salahuddin, *Nano Lett.* **2011**, *11*, 3768.
[36] B. Radisavljevic, A. Radenovic, J. Brivio, V. Giacometti, A. Kis, *Nat. Nanotechnol.* **2011**, *6*, 147.
[37] A. Rai, A. Valsaraj, H. C. Movva, A. Roy, R. Ghosh, S. Sonde, S. Kang, J. Chang, T. Trivedi, R. Dey, S. Guchhait, S. Larentis, L. F. Register, E. Tutuc, S. K. Banerjee, *Nano Lett.* **2015**, *15*, 4329.
[38] H. Ji, H. Yi, S. Wonkil, H. Kim, S. C. Lim, *Nanotechnology* **2019**, *30*, 345206.
[39] A. Rai, H. Movva, A. Roy, D. Taneja, S. Chowdhury, S. Banerjee, *Crystals* **2018**, *8*, 316.
[40] M. Siao, W. Shen, R. Chen, Z. Chang, M. Shih, Y. Chiu, C. Cheng, *Nat. Commun.* **2018**, *9*, 1442.
[41] R. Dagan, Y. Vaknin, A. Henning, J. Shang, L. Lauhon, Y. Rosenwaks, *Appl. Phys. Lett.* **2019**, *114*, 101602.
[42] M. Heyl, D. Burmeister, T. Schultz, S. Pallasch, G. Ligorio, N. Koch, E. J. W. List-Kratochvil, *Phys. Status Solidi RRL* **2020**, *14*, 2000408.
[43] J. Shim, S. H. Bae, W. Kong, D. Lee, K. Qiao, D. Nezich, Y. J. Park, R. Zhao, S. Sundaram, X. Li, H. Yeon, C. Choi, H. Kum, R. Yue, G. Zhou, Y. Ou, K. Lee, J. Moodera, X. Zhao, J. H. Ahn, C. Hinkle, A. Ougazzaden, J. Kim, *Science* **2018**, *362*, 665.